Proceedings of the
Annual Stability Conference
Structural Stability Research Council
Pittsburgh, Pennsylvania, May 10-14, 2011

Behavior and design of cold-formed steel lipped and plain angles

Y.Shifferaw[1], B.W.Schafer[2]

Abstract

The objective of this study is to explore the significant post-buckling reserve in global buckling that has been observed in testing of cold-formed steel angles, and to provide design guidance for locally slender cold-formed steel lipped and plain angles with fixed end boundary conditions. Global buckling modes are generally regarded to have no post-buckling reserve, and indeed all column design curves, including those used in AISI-S100 for cold-formed steel columns limit the strength to $0.877P_{cr}$ (where P_{cr} is the global buckling load) or lower. However, tests conducted on cold-formed steel angles by Young and his students (Young [2004, 2005] and Young et al. [2005, 2007]) demonstrate capacities significantly in excess of P_{cr} – an observation usually observed in local-plate buckling modes, which due to the nature of the deformations have significant post-buckling reserve. This research builds upon previous work on cold-formed steel angles that demonstrated the "overlap" between local-plate and global torsional buckling modes in cold-formed steel angles. In this work specific attention is paid to some unique aspects of cold-formed steel angles under compression: (1) the separation, or lack of, between local-plate and global torsional buckling, and (2) the specific impact of end boundary conditions, with particular emphasis on warping (longitudinal) deformations. Utilizing nonlinear collapse analysis with shell finite element models, and existing testing, alternatives to current design methods are explored. Given the end boundary conditions are known, new design procedures are recommended for strength prediction of cold-formed steel angles.

Introduction

Angles are one of the simplest cold-formed steel cross-sections to form, yet their behavior and design is anything but simple. For example, identifying and separating the local and global elastic critical buckling modes, particularly for plain angles, is not straightforward.

For strength prediction of axially loaded, simply supported slender angles, Rasmussen [2003, 2005] utilized an effective width approach including consideration for eccentricity due to shift of the centroid in the effective section. The approach results in a full beam-column design even for concentrically loaded angles. Rasmussen [2006] extended this approach to the Direct Strength Method (DSM) for plain equal leg angles subjected to compression by ignoring global torsional

[1] Post-doctoral Research Scholar, Civil Engineering, Johns Hopkins University, <yaredshi@jhu.edu>
[2] Professor and Chair, Civil Engineering, Johns Hopkins University, <schafer@jhu.edu>

buckling and considering only local-plate and flexural buckling in the design predictions. Note, the need to consider shift in the effective centroid is greatest for pinned end conditions, as shift in eccentricity is limited in the case of fixed end boundary conditions. Chodraui et al. [2006] recommended a simplified DSM approach, not taking into consideration any explicit shift in eccentricity, and treating the overlapping "torsion" mode as both a local-plate and global mode.

Experiments conducted on concentrically loaded angles with fixed end boundary conditions resulted in significant variation in the strength capacities when compared against global flexural-torsional buckling. The tests of Young [2004, 2005] and Young et al. [2005, 2007] revealed strengths greatly in excess of current design specifications (e.g., AISI-S100-07) and surprising post-buckling strength.

This study investigates how DSM for angles may be formulated to address the overlapping nature of the local-plate and global modes and examines the current approach in the treatment of the elastic critical buckling modes related to plain angles. Further, this study explores the behavior of plain and lipped angles with fixed end boundary conditions. Shell finite element (FE) eigen- and post-buckling analyses are used to classify the behavior and propose DSM extensions to angles with fixed end boundary conditions.

Background

Elastic stability of angles in compression: Effect of lip on local buckling

A small parametric study is completed to illustrate the impact of the presence of lips on the elastic critical buckling of angles. A summary of the elastic buckling analyses using the finite strip method implemented in CUFSM 3 (Schafer and Ádány [2006]) for varying lip ratios (as a percent of angle leg length) for an equal leg angle (leg = 2.89 in., thickness = 0.059 in., and yield stress=84.18 ksi.) is provided in Figure 1.

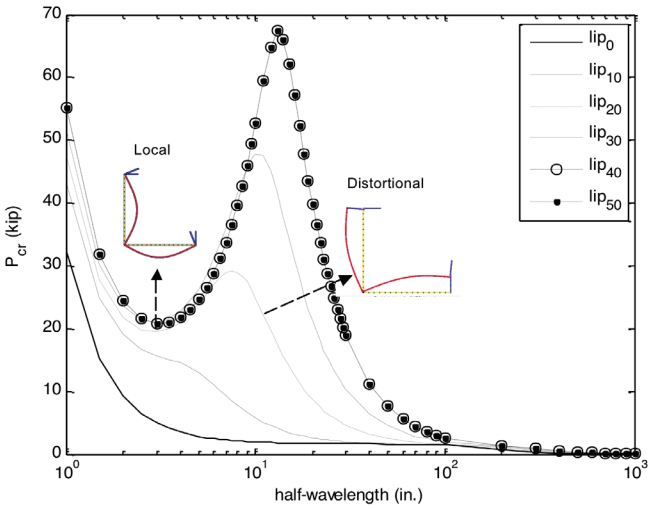

Figure 1 Effect of lip on elastic critical buckling by finite strip analysis

Local-plate modes with distinct critical minima are observed for angles with lip ratios greater than 20%. In these sections, the distortional buckling mode is also observed; however there is no distinct distortional minimum. For a short range, beyond the half-wavelength where the local mode dominates, distortional buckling controls. At intermediate lengths global torsion generally

controls, while for longer lengths, global flexure dominates. As the lip size decreases (lip ratio less than 20%), the local and distortional boundary disappears.

For a plain angle subjected to compression the mode shapes for local-plate and global torsional buckling are similar, and mathematically coincident as described in Rasmussen [2003], rendering great difficulty in the classification of the elastic critical buckling modes.

Effect of boundary conditions on elastic stability

A comparison of analytical and numerical methods on the impact of boundary conditions for elastic critical global buckling of lipped angles subjected to compression is provided. Simply support and fixed end boundary conditions, with warping free and fixed cases, are considered.

Eigen FE models for pinned end boundary conditions: locally warping free and warping fixed

To determine the elastic critical buckling failure for pinned angles with warping fixed and warping free boundary conditions shell FE eigen-buckling analysis using ABAQUS [2007] is undertaken. For a warping free FE model with pin-pin boundary conditions, equivalent nodal loads obtained from a finite strip analysis via CUFSM are applied. The loaded end is restrained from translations except in the longitudinal direction. In the center at mid-length a single point is restrained in the longitudinal direction. For pin-pin boundary conditions with warping fixity the ends are subjected to a unit longitudinal displacement at a reference node located at the geometric centroid of the section, while all other end translations are restricted, along with longitudinal translation of a single point at mid-length.

Comparison with CUFSM and CUTWP for pinned end boundary condition

A comparison of eigen-buckling results for ABAQUS FE models with classical beam theory expressions of CUTWP (Sarawit [2006]) and the semi-analytical finite strip method for pin-pin end boundary conditions of CUFSM (Schafer and Ádány [2006]) is provided in Table 1 for the L1.5L2500 section (see Table 3 for dimensions, L = 2500 mm = 98.4 in.) in compression. For pin-pin warping free conditions all methods agree. Pin-pin warping-fixed conditions have a significant impact on the effective length in torsion (KL_3). Assuming the fix-fix effective length in torsion: $KL_3 = 0.5L$ for classical (CUTWP) P_{cr}, is close to the ABAQUS (FE) results, but slightly unconservative. Presumably the effective length for St. Venant torsion is not at 0.5L, while the warping torsion is at a KL of 0.5L. Through back-calculation $KL_3 = 0.527L$ is found to have excellent agreement with the FE model (but this is cross-section and length dependent).

Table 1 Elastic critical buckling values for pinned ends via computational tools for L1.5L2500

Method	P_{cr} (kips)	
	Pin-Pin Warping free	Pin-Pin Warping fixed
ABAQUS	1.67	2.71
CUTWP	1.68[a]	2.71[b] 2.87[c]
CUFSM	1.68[d]	-

(a) $KL_1=KL_2=KL_3=L$
(b) $KL_1=KL_2=L;KL_3=0.527L$
(c) $KL_1=KL_2=L;KL_3=0.5L$
(d) CUFSM 3 (Schafer and Ádány 2006)

Eigen FE models for fixed boundary conditions: locally warping free and warping fixed
To simulate a fixed, warping free boundary condition, compression is applied through direct loading. All end displacements, except longitudinal translation, are restrained. For fixed end, warping fixed, boundary conditions all end nodes are tied to a reference node at the centroid. A unit displacement is applied at the reference node and all other translations and rotations are restrained at the reference node.

Comparison with CUFSM and CUTWP for fixed boundary conditions
As provided in Table 2, for fixed ends with warping fixity ABAQUS, CUTWP, and CUFSM (in this case CUFSM 4 (Li and Schafer [2010])) provide essentially the same solution. For fixed ends without warping fixity (warping free) the elastic buckling load is lower than pinned ends with warping fixity (see Table 1) highlighting the importance of warping fixity on angle stability. For the fixed end, warping free case, assuming flexure is fixed $KL_1=KL_2=0.5L$ and twist pinned $KL_3=L$ is overly conservative; and instead $KL_3=0.75L$ is found to provide the best agreement. Thus, again the interplay between St. Venant (warping insensitive) and warping torsion in twist, is observed.

Table 2 Elastic critical buckling values for fixed ends via computational tools for L1.5L2500

Method	P_{cr} (kips)	
	Fixed-Fixed Warping free	Fixed-Fixed Warping fixed
ABAQUS	2.06	3.01
CUTWP	2.07[a] 1.73[b]	3.03[c]
CUFSM	-	3.08[d]

(a) $KL_1=KL_2=0.5L$; $KL_3=0.75L$
(b) $KL_1=KL_2=0.5L$; $KL_3=L$
(c) $KL_1=KL_2=KL_3=0.5L$
(d) CUFSM 4 (Li and Schafer 2010)

Existing Tests on Plain and Lipped Angles

Summary of Existing Tests
Geometric and material properties of the angles in the fixed-ended tests of Young [2004, 2005] are given in Table 3. Figure 2 provides a plot of normalized capacity as a function of specimen length for Young's tests. Specimen designation, such as L1.5L2500 implies the L1.5 cross-section (Table 3) with a length L = 2500 mm (98.4 in.). The L series are for equal leg lipped angles, and the P series for equal leg plain angles.

Table 3 Average geometric and material properties of fixed ended tests of Young [2004, 2005]

Specimen group	leg (in.)	lip (in.)	t (in.)	f_y (ksi)	r_i (in.)	f_u (ksi)	ε_u (%)	E (ksi)
L1.2	2.85	0.67	0.047	84.1	0.102	86.3	9	30603
L1.5	2.89	0.66	0.059	73.2	0.102	79.8	11	30748
L1.9	2.90	0.70	0.074	71.8	0.102	77.6	10	30893
P1.2	2.82	-	0.046	79.8	0.102	83.4	10	30168
P1.5	2.81	-	0.059	76.9	0.102	79.8	11	30023
P1.9	2.83	-	0.074	72.5	0.102	76.9	11	30168

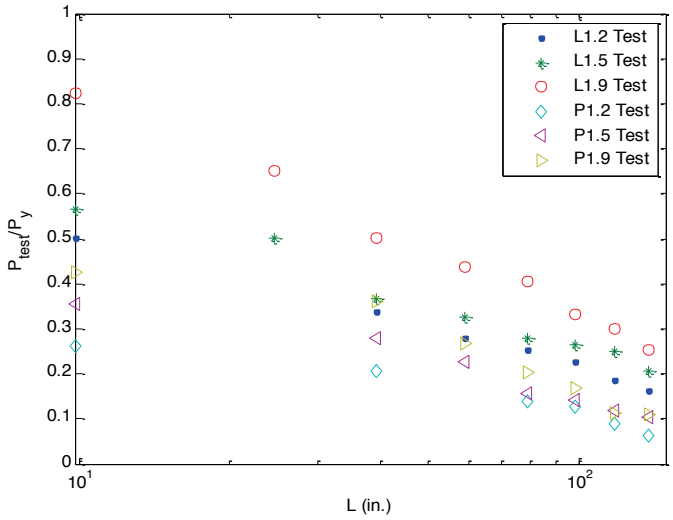

Figure 2 Normalized compressive strengths of tested angles possessing post-buckling reserve

Nonlinear FE collapse models

Validation of model against test data

Shell FE models of Young's tests (Table 3, Figure 2) are created with fixed end, warping fixed boundary conditions meshed with ABAQUS S9R5 shell elements with an average aspect ratio of 1 and inside the range of 1 to 4 for all elements. Geometry is based on Table 3, but with sharp corners. Geometric imperfections consistent with Type I and Type II imperfections at 50% probability of exceedance (0.34t and 0.94t respectively) from Schafer and Peköz [1998] are employed. The material is modeled as elasto-plastic (f_y, f_u, ε_u from Table 3) and converted to true stress-strain. The yield criterion is von Mises and hardening is isotropic. The arc-length method is used for nonlinear solution control in the static analyses. For the L1.5 series the test and FE collapse analysis predictions are provided in Figure 3 and Table 4. The average test to predicted load is 0.93 with a standard deviation of 0.05, indicating that the tests (and boundary conditions) are reasonably well-represented by the FE model.

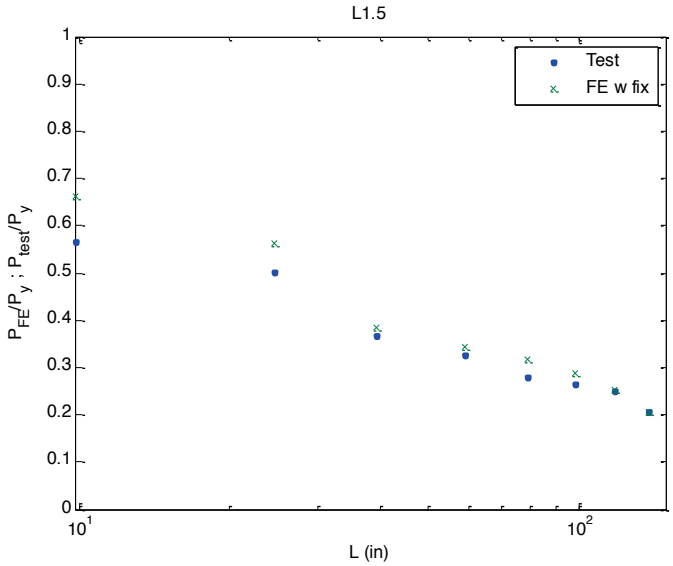

Figure 3 Finite element analysis results vs. tests for a lipped angle L1.5 series

Table 4 Test results vs. FE model predictions for L1.5 angles

Specimen	P_{test}*	P_{FE}	P_{test}/P_{FE}
L1.5L250	19.02	22.18	0.86
L1.5L625	16.84	18.88	0.89
L1.5L1000	12.34	12.85	0.96
L1.5L1500	10.95	11.52	0.95
L1.5L2000	9.33	10.59	0.88
L1.5L2500	8.86	9.64	0.92
L1.5L3000	8.39	8.50	0.99
L1.5L3500	6.95	6.91	1.01
		Average	0.93

* Young (2004, 2005)

Post-buckling capacity and collapse models as a function of boundary conditions: Sensitivity of post-buckling to warping restraint

The sensitivity of the strength to end boundary conditions is illustrated for the L1.5 test series in Figure 4. Only the nonlinear collapse models with fixed ends and warping fixed (FE w fix in Figure 4) agree with the tests. If warping fixity is released (FE w free) or the ends are pinned (FE simple s) the strength is far below the test.

Figure 4 also demonstrates the remarkable post-buckling capacity in Young's tests. The test strength is far above the flexural-torsional elastic buckling solution (for L > 40 in.) Note, this is not typical as for pinned-ends the FE collapse models and the elastic buckling solution are, as expected, in exact agreement. The post-buckling performance is illustrated more directly in Figure 5, which provides the axial load (P_1) normalized by the buckling load (P_{cr}) vs. the axial displacement (U_{11}) for the FE collapse simulations of the L1.5 test series.

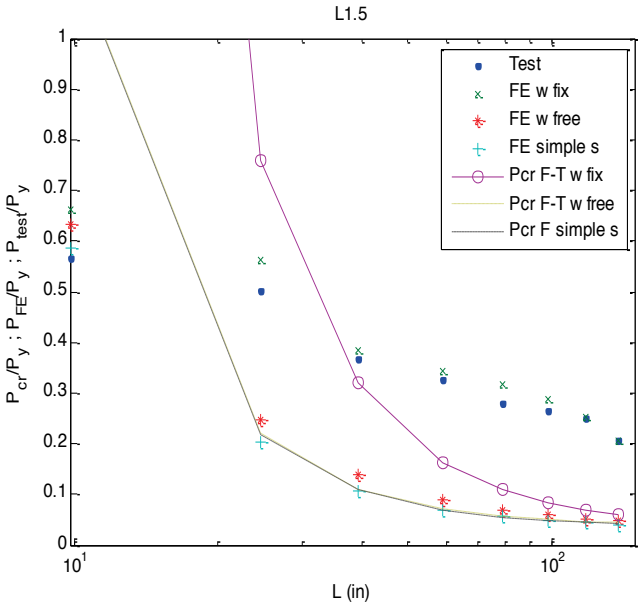

Figure 4 Effect of boundary conditions on collapse FE models for lipped angle L1.5 test series

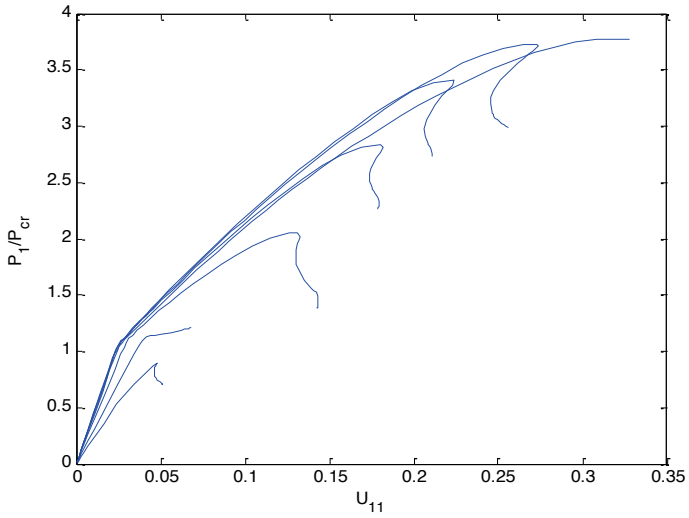

Figure 5 Normalized FE collapse load vs. displacement for warping fixed lipped angle L1.5

Design of cold-formed steel angles

Exploring Direct Strength Method approaches for strength prediction: lipped angles

As implemented, DSM provides no post-buckling in global modes (AISI-S100-07 Appendix 1, Schafer [2008]). However, for lipped angles with warping fixed end conditions in global modes dominated by torsion post-buckling is observed. Three options for capturing the increased strength in global buckling (P_{ne}) of lipped angles with warping fixity are considered.

Option 1: No post-buckling, no change to P_{ne}

For $\lambda_c \le 1.5$ $$P_{ne,g} = 0.658^{\lambda_c^2} P_y \quad (1)$$

$\lambda_c > 1.5$ $$P_{ne,g} = \frac{0.877}{\lambda_c^2} P_y \quad (2)$$

where $\lambda_c = \sqrt{P_y / P_{cre}}$, and P_{cre} = minimum critical elastic global buckling load

Option 2: Use "local DSM" post-buckling curve, with transition for P_{ne}

For $\lambda_c \le 1.446$ $$P_{ne,\ell} = 0.820^{\lambda_c^2} P_y \quad (3)$$

$\lambda_c > 1.446$ $$P_{ne,\ell} = \left(1 - 0.15\left(\frac{P_{cre,FT}}{P_y}\right)^{0.4}\right)\left(\frac{P_{cre,FT}}{P_y}\right)^{0.4} P_y \quad (4)$$

where $\lambda_c = \sqrt{P_y / P_{cre,FT}}$, and $P_{cre,FT}$ = critical elastic flexural-torsional buckling load

Option 3: Use "distortional DSM" post-buckling curve, with transition for P_{ne}

For $\lambda_c \le 1.264$ $$P_{ne,d} = 0.735^{\lambda_c^2} P_y \quad (5)$$

$\lambda_c > 1.264$ $$P_{ne,d} = \left(1 - 0.25\left(\frac{P_{cre,FT}}{P_y}\right)^{0.6}\right)\left(\frac{P_{cre,FT}}{P_y}\right)^{0.6} P_y \quad (6)$$

where $\lambda_c = \sqrt{P_y / P_{cre,FT}}$ and $P_{cre,FT}$ = critical elastic flexural-torsional buckling load

The global strength prediction options need to be combined with local ($P_{n\ell}$), and distortional (P_{nd}) strength predictions to provide a full prediction method as given in Table 5. The resulting strength predictions are designated as P_{n_1}, P_{n_2}, and P_{n_3} as given in Table 5.

Table 5 Options for application of the Direct Strength Method to lipped angles

Nominal strength	1	2	3
P_{ne}	$P_{ne,g}=f(\min(P_{cr,FT},P_{cr,F}),P_y)$	$P_{ne,\ell}=f(P_{cr,FT},P_y)$	$P_{ne,d}=f(P_{cr,FT},P_y)$
$P_{n\ell}$	$P_{n\ell}=f(P_{cr\ell},P_{ne,g})$	$P_{n\ell}=f(P_{cr\ell},P_{ne,\ell})$	$P_{n\ell}=f(P_{cr\ell},P_{ne,d})$
P_{nd}	$P_{nd}=f(P_{crd},P_y)$	$P_{nd}=f(P_{crd},P_y)$	$P_{nd}=f(P_{crd},P_y)$
P_n	$P_{n_1}=min(P_{ne,g}, P_{nl}, P_{nd})$	$P_{n_2}=min(P_{ne,l}, P_{nl}, P_{nd})$	$P_{n_3}=min(P_{ne,d}, P_{nl}, P_{nd})$

Comparison of P_{n_1}, P_{n_2}, and P_{n_3} strength predictions with the lipped angles (L1.2, L1.5 and L1.9) test series is provided in Figure 6. Ignoring post-buckling (P_{n_1}) is excessively conservative, assuming global torsional post-buckling is identical to local-plate post-buckling (P_{n_2}) is unconservative, while assuming global torsional post-buckling is similar to distortional post-buckling (P_{n_3}) provides reasonably good agreement. The test-to-predicted ratio for P_{n_3} is 1.07 with a standard deviation of 0.16, which may be compared with the test-to-predicted ratio of the existing expression (P_{n_1}) which is 2.37 with a standard deviation of 1.17! When lipped angle warping fixity is provided (e.g., from welded ends) the P_{n_3} approach is recommended.

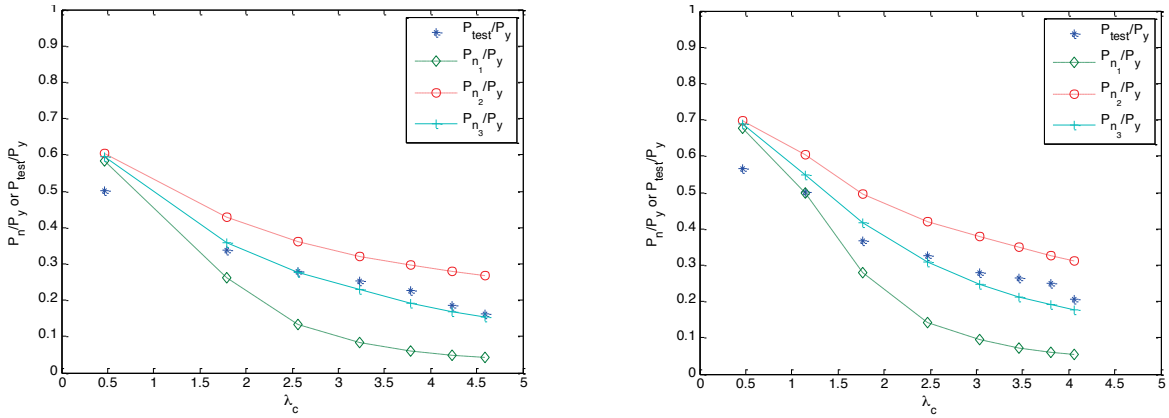

(a)L1.2 series

(b) L1.5 series

(c) L1.9 series

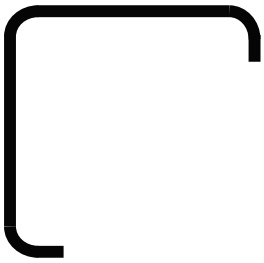

(d) lipped equal leg angle

Figure 6 Normalized nominal strengths vs. slenderness for DSM options in warping-fixed equal-lipped angles

Exploring Direct Strength Method approaches for strength prediction: plain angles

Plain angles are essentially a degenerate case for the characterization of elastic buckling modes. Therefore, as Table 6 shows, a variety of methods exist for mapping known elastic buckling solutions of local-plate (L), global torsional (T) and global flexural (F) buckling to the elastic global (P_{cre}), distortional (P_{crd}) and local ($P_{cr\ell}$) buckling loads needed for DSM analysis.

Table 6 Options for application of the Direct Strength Method to plain angles*

	a	b	c	d	e	f
P_{cre}	*min(L/T,F)*	*F*	*F*	*min(L/T,F)*	*min(L/T,F)*	*min(L/T,F)*
P_{crl}	*L/T*	*L/T*	*L/T*	-	*L/T*	*L/T=F*
P_{crd}	-	-	*L/T*	-	*L/T*	-

*See also discussed in Chodraui et al. [2006]

In addition, two options for the global strength curve of plain angles are considered.

Option 1: No change to global curve

$$\text{For } \lambda_c \le 1.5 \qquad P_{ne,g1} = 0.658^{\lambda_c^2} P_y \tag{7}$$

$$\lambda_c > 1.5 \qquad P_{ne,g1} = \frac{0.877}{\lambda_c^2} P_y \tag{8}$$

where $\lambda_c = \sqrt{P_y / P_{cre}}$ and P_{cre} = critical elastic global bucking load per Table 6

Option 2: Reduced global curve

$$\text{For } \lambda_c \le 1.106 \qquad P_{ne,g2} = 0.40^{\lambda_c^2} P_y \tag{9}$$

$$\lambda_c > 1.106 \qquad P_{ne,g2} = \frac{0.40}{\lambda_c^2} P_y \tag{10}$$

where $\lambda_c = \sqrt{P_y / P_{cre}}$ and P_{cre} = critical elastic global bucking load per Table 6

Design methods following the options of Table 6 and the two global curves for P_{ne} are compared with the fixed end plain angle (P1.2, P1.5 and P1.9) test series in Figure 7. First, note that the use of option a (or d, e, or f) where P_{cre} is the minimum of L/T and F yields a strength prediction far below the tests and one that is independent of the flexural (F) slenderness. This is inconsistent with both the observed strength and trend in the data – thus the use of flexure only (F) for P_{cre} as earlier recommended by Rasmussen is strongly supported in this data. It is worth noting that from the perspective of the global-torsional mode significant post-buckling strength is observed in these plain angle fixed-end tests similar to the lipped angle tests; however, in plain angles the insensitivity of P_{cre} based on global-torsion to length, makes it essentially impossible to use this parameter in an acceptable design method.

The use of the existing DSM expressions and option b for defining the elastic buckling loads ($P_{nDSM1(b)}$) follows the trend of the data well (in Figure 7) but is slightly unconservative. The local buckling reduction down to $P_{n\ell}$ from P_{ne} is important (compare to flexure only cases in Figure 7) but the observed strength is still below the predictions. A possible alternative is presented in $P_{nDSM2(b)}$ where the global curve is further reduced (Option 2 of Eq.'s 9 and 10).

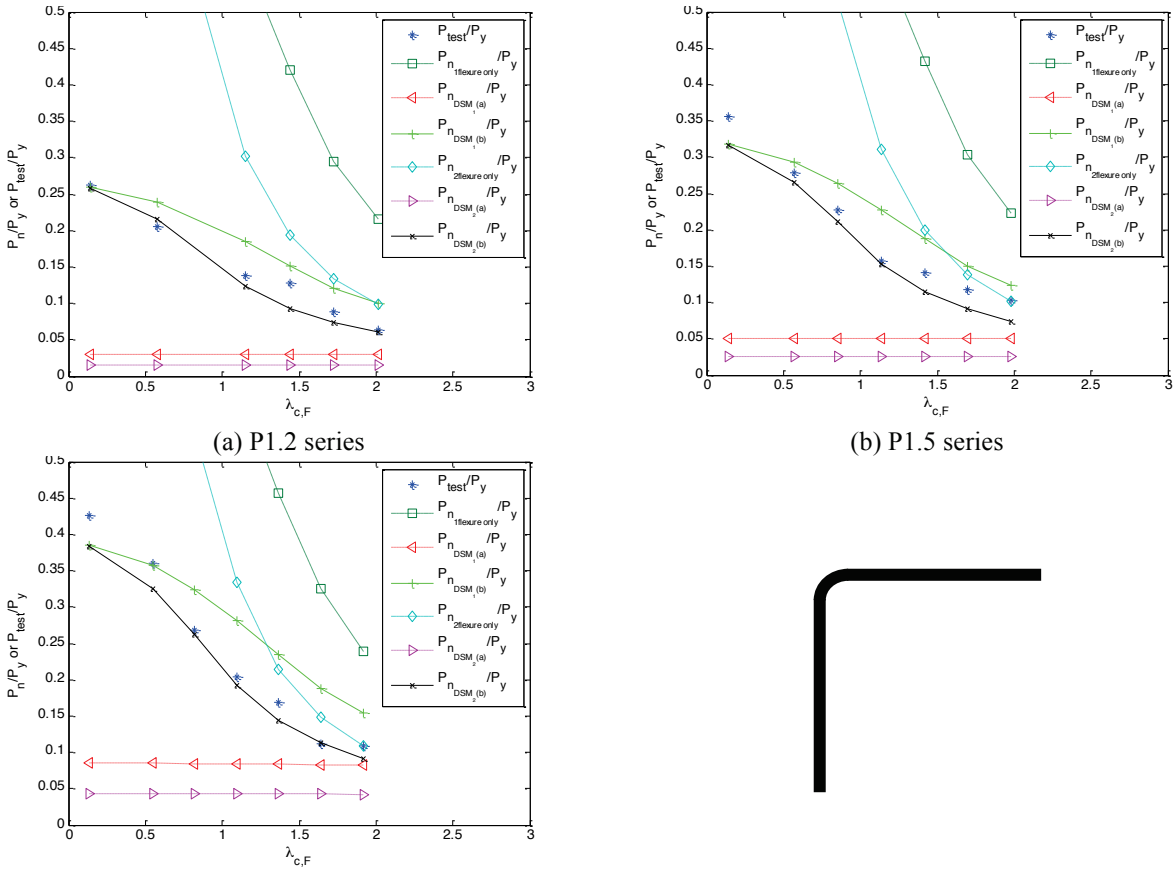

(a) P1.2 series

(b) P1.5 series

(c) P1.9 series

(d) plain equal leg angle

Figure 7 Normalized nominal strengths vs. slenderness for DSM options in warping-fixed plain angles

Discussion

Despite advances, angles still provide great difficulty for semi-empirical design methods that attempt to classify buckling modes and utilize strength curves associated with those modes. In particular, lipped and plain angles exhibit a strong sensitivity to warping boundary conditions. More importantly, this sensitivity extends not only in the elastic buckling regime, but to the post-buckling regime as well. The surprise is how beneficial the warping fixity is, not only in boosting the buckling load, but in also creating the conditions for post-buckling in torsion dominated global modes. Further studies related to the strength of angles may be found in Shifferaw (2010).

Conclusions

Existing experiments combined with elastic buckling analysis demonstrate that plain and lipped angles with fixed end conditions exhibit post-buckling with respect to global torsional (plain angle) or flexural-torsional (lipped angle) buckling modes. This post-buckling is ignored in all current design methods for cold-formed steel plain or lipped angles. The importance of warping fixity in torsion of angles is highlighted through eigen-buckling analysis and nonlinear shell finite element collapse analysis. For lipped angles with fixed ends (including warping) a new global column curve (for use in DSM or effective width methods), including post-buckling, is developed and shown to provide reasonable strength predictions. For plain angles with fixed ends torsional post-buckling is accounted for by including torsion only in local buckling, thereby

assuming the global torsional strength (with post-buckling) always exceeds the global flexural strength. Ignoring global torsion and replacing with global flexure in fixed end plain angles must be done with some care for conservative results, and a reduced column curve is explored. Work remains to develop a definitive design method for cold-formed steel angles; however, the influential role of warping restraint provides the best avenue for additional exploration.

Acknowledgments

The authors of this work would like to acknowledge the National Science Foundation for supporting this work under Grant No. 0448707 and Ben Young for the invaluable discussion and recommendations leading to this research. Only the authors' views, and not necessarily those of the NSF, are reflected in the material presented.

References

ABAQUS. (2007). *ABAQUS/Standard User's Manual*, Version 6.7, ABAQUS, Inc., Pawtucket, RI.

AISI-S100. (2007). *North American Specification for the Design of Cold-Formed Steel Structural Members*, American Iron and Steel Institute, Washington, D.C.

Chodraui, G.M.B., Shifferaw, Y., Malite, M., Schafer, B.W. (2006). "Cold-formed steel angles under axial compression." *Proceedings of the Eighteenth International Specialty Conference on Cold-Formed Steel Structures*, Orlando, FL. October 2006. 285-300.

Li, Z., Schafer, B.W. (2010). "Buckling analysis of cold-formed steel members with general boundary conditions using CUFSM: conventional and constrained finite strip methods." *Proceedings of the Twentieth International Specialty Conference on Cold-Formed Steel Structures*, St. Louis, MO. 17-32.

Rasmussen, K.J.R. (2003). "Design of angle columns with locally unstable legs." *Department of Civil Engineering, Research Report No. R830, University of Sydney*. Australia.

Rasmussen, K.J.R. (2005). "Design of angle columns with locally unstable legs." ASCE, *J. Struct. Eng.*, 131 (10) 1553-1560.

Rasmussen, K.J.R. (2006). "Design of slender angle section beam-columns by the direct strength method." ASCE, *J. Struct. Eng.*, 132 (2) 204-211.

Sarawit, A. (2006). "CUTWP Thin-walled section properties." Version 2003, accessed at www.ce.jhu.edu/bschafer/cutwp.

Schafer, B.W. (2008). "Review: The Direct Strength Method of cold-formed steel member design." *J. Constr. Steel Res.*, 64(7-8), 766-778.

Schafer, B.W., Ádány, S. (2006). "Buckling analysis of cold-formed steel members using CUFSM: conventional and constrained finite strip methods." *Proceedings of the Eighteenth International Specialty Conference on Cold-Formed Steel Structures*, Orlando, FL. 39-54.

Schafer, B.W., Peköz, T. (1998). "Computational modeling of cold-formed steel: characterizing geometric imperfections and residual stresses." Elsevier, *J. Constr. Steel Res.*, 47 (3), 193-210.

Shifferaw, Y. (2010). "Section capacity of cold-formed steel members by the Direct Strength Method." Ph.D. thesis, The Johns Hopkins University, Baltimore, Maryland.

Young, B. (2004). "Tests and design of fixed-ended cold-formed steel plain angle columns." ASCE, *J. Struct. Eng.*, 130(12), 1931-1940.

Young, B. (2005). "Experimental investigation of cold-formed steel lipped angle concentrically loaded compression members." ASCE, *J. Struct. Eng.*, 131(9), 1390-1396.

Young, B., Ellobody, E. (2005). "Buckling analysis of cold-formed steel lipped angle columns." ASCE, *J. Struct. Eng.*, 131(10), 1570-1579.

Young, B., Ellobody, E. (2007). "Design of cold-formed steel unequal angle compression members." Elsevier, *Thin-Walled Struct.*, 45, 330-338.